

## Diphoton + jets at NLO

---

**Thomas Gehrmann**

*Institute for Theoretical Physics, University of Zürich, Winterthurerstrasse 190, CH-8057  
Zürich, Switzerland*

*E-mail: [thomas.gehrmann@uzh.ch](mailto:thomas.gehrmann@uzh.ch)*

**Nicolas Greiner\***

*Max Planck Institute for Physics, Föhringer Ring 6, D-80805 München, Germany*

*E-mail: [greiner@mpp.mpg.de](mailto:greiner@mpp.mpg.de)*

**Gudrun Heinrich**

*Max Planck Institute for Physics, Föhringer Ring 6, D-80805 München, Germany*

*E-mail: [gudrun@mpp.mpg.de](mailto:gudrun@mpp.mpg.de)*

We present the next-to-leading order QCD corrections to the production of a photon pair in association with one or two jets. This class of processes constitutes an important background for Higgs physics at the LHC. For the one jet process we include photon fragmentation contributions and perform a comparison between different photon isolation criteria and various isolation parameters. The two jet calculation has been performed using a smooth cone isolation criterion. We find that the NLO QCD corrections are substantial and can lead to distortions of differential distributions.

*11th International Symposium on Radiative Corrections (Applications of Quantum Field Theory to Phenomenology)*

*22-27 September 2013*

*Lumley Castle Hotel, Durham, UK*

---

\*Speaker.

## 1. Introduction

The production of a photon pair at the LHC within the Standard Model is an important background for the Higgs boson observed at the LHC [1]. One of the most important decay channels is the decay into a photon pair [5, 3, 2], due to its clean signature. The Standard Model background, the production of two photons without an intermediate Higgs, is experimentally determined by means of sideband subtraction. However, for a more precise determination of the Higgs parameters, this estimation of the background might not be precise enough. Therefore it is crucial to have a reliable theoretical prediction for this class of processes. The production of two photons is known fully differentially at NLO [6], including gluon initiated subprocesses [9] and resummation effects [10, 11]. Recently also the NNLO result has become available [7].

The presence of extra jets allows for a better control of the backgrounds and for a distinction of different Higgs production processes. In particular, the additional production of two jets allows to probe the vector boson fusion production mechanism. Therefore the QCD corrections for processes with the presence of extra jets are an important ingredient for reliable predictions in the diphoton plus jets channel. The production of a photon pair in association with one jet is known at NLO [8] using a smooth cone isolation criterion [12]. We present an NLO QCD calculation for diphoton plus one jet where for the first time different photon isolation criteria and different isolation parameters are compared, and we present the first NLO calculation of diphoton plus two-jet production.

## 2. Photon isolation and photon fragmentation

A final state photon can either originate from the hard scattering matrix elements which means it is perturbatively accessible, or it can originate from the fragmentation of hadrons into photons. The latter production mechanism is of non-perturbative nature and therefore can not be described using a fixed order calculation. Only the production of photons from the hard interaction can be computed within perturbation theory from first principles, while the production of photons in hadronization and hadron decays can only be modeled, thereby introducing a dependence on rather poorly known fragmentation parameters.

The characteristics of the photon typically depend on its origin. Secondary photons, i.e. photons stemming from hadronic decays, are usually inside a jet cone formed by the hadrons. Photons coming from the hard interaction tend to be separated from hadronic jets. In order to distinguish the two types, one applies photon isolation cuts, which limit the hadronic activity around a photon candidate. However, a veto on all hadronic activity around the photon direction would result in a suppression of soft gluon radiation in part of the final state phase space, thereby violating infrared safety of the observables. Consequently, all photon isolation prescriptions must admit some residual amount of hadronic activity around the photon direction. In the following we focus on two types of photon isolation. One is the cone-based isolation which is most commonly used at hadron collider experiments. In this procedure, the photon candidate is identified (prior to the jet clustering) from its electromagnetic signature, and its momentum direction (described by transverse energy  $E_{T,\gamma}$ , rapidity  $\eta_\gamma$  and polar angle  $\phi_\gamma$ ) is determined. Around this momentum direction, a cone of radius  $R_\gamma$  in rapidity  $\eta$  and polar angle  $\phi$  is defined. Inside this cone, the hadronic trans-

verse energy  $E_{T,\text{had}}$  is measured. The photon is called isolated if  $E_{T,\text{had}}$  is below a certain threshold, defined either in absolute terms, or as a fraction of  $E_{T,\gamma}$ . The latter criterion then means that a photon candidate is considered as isolated if it fulfills the condition

$$E_{\text{had,cone}} \leq \varepsilon_c p_T^\gamma, \quad (2.1)$$

inside the cone with radius  $R$ . The cone-based isolation allows events with a quark being collinear to a photon. The theoretical predictions for cross sections defined with this type of isolation must therefore take account of photon fragmentation contributions.

A different option is the smooth cone isolation [12]. It varies the threshold on the hadronic energy inside the isolation cone with the radial distance from the photon. It is described by the cone size  $R_\gamma$ , a weight factor  $n_\gamma$  and an isolation parameter  $\varepsilon_\gamma$ . With this criterion, one considers smaller cones of radius  $r_\gamma$  inside the  $R_\gamma$ -cone and calls the photon isolated if the energy in any sub-cone does not exceed

$$E_{\text{had,max}}(r_\gamma) = \varepsilon_\gamma p_T^\gamma \left( \frac{1 - \cos r_\gamma}{1 - \cos R_\gamma} \right)^{n_\gamma}. \quad (2.2)$$

By construction, the smooth cone isolation does not admit any hard collinear quark-photon configurations, thereby allowing a full separation of direct and secondary photon production, and consequently eliminating the need for a photon fragmentation contribution in the theoretical description. Despite its theoretical advantages, the smooth cone isolation was up to now used in experimental studies of isolated photons only in a discretized approximation. Experimentally, owing to finite detector resolution, the implementation of this isolation criterion will always require some minimal, nonzero value of  $r_\gamma$ , thereby leaving potentially a residual collinear contribution.

### 3. Diphoton + one jet

A detailed calculation of this process and a comparison between the two photon isolation types can be found in [13]. The code that has been used to produce the presented results has been made public and can be downloaded from <https://gosam.hepforge.org/diphoton/>.

#### 3.1 Setup of the calculation

Both the calculation of diphoton plus one jet as well as with two jets, described in section 4, are performed using the same setup. For the generation of the tree level and real emission matrix elements we use MadGraph [14], the regularization of infrared QCD singularities is handled by MadDipole [15], which makes use of the dipole formalism as developed in Ref. [16]. For integration over the phase space we used MadEvent [17]. The routines for generating histograms and distributions originate from the MadAnalysis package (see <http://madgraph.hep.uiuc.edu>). All ingredients are generated and combined in a fully automated way.

The virtual amplitudes have been obtained using GoSam [18], a public package for the automated generation of one-loop amplitudes. It uses Qgraf [19], FORM [20] and Spinney [21] for the generation of the amplitudes, which are optimized and written as a Fortran90 code with the use of Haggies [22]. For the reduction of the one-loop amplitudes we used Samurai [23], which performs

a reduction at the integrand level based on the OPP-method [24]. As a rescue for numerically unstable points, the tensor reduction method of the Golem95 library [25] has been used. The remaining master integrals are computed with either OneLoop [26], or Golem95 [25].

In the case where the fixed cone isolation is used, the real emission contribution contains infrared singularities related to the collinear emission of the photon off a final-state QCD parton. They need to be regularized by some kind of subtraction terms. The corresponding integrated subtraction terms make this singularity apparent as they contain an explicit pole term when integrating over the unresolved one-particle phase space in dimensional regularization. This pole is then absorbed into the fragmentation functions. To regulate these singularities we again make use of the dipole formalism as developed in Ref.[27] and implemented in the QED extension of MadDipole [28]. This extension also offers the framework for a straightforward implementation of fragmentation functions.

### 3.2 Numerical Results

For the results presented here we assumed as center of mass energy of  $\sqrt{s} = 8$  TeV and we employed a set of basic cuts:  $p_T^{\text{jet}} > 40$  GeV,  $p_T^\gamma > 20$ ,  $|\eta^\gamma, \eta^j| \leq 2.5$ ,  $100 \text{ GeV} \leq m_{\gamma\gamma} \leq 140$  GeV. For the jet clustering we used an anti- $k_T$  algorithm [29] with a cone size of  $R = 0.4$  provided by the FastJet package [30]. We used an NLO pdf set from NNPDF2.3 [31], where the values for  $\alpha_s$  at leading order and next-to-leading order are given by  $\alpha_s(M_Z) = 0.119$ . For the photon fragmentation functions, we take set II of the parametrisations of Ref. [32]. Renormalization and factorization scales  $\mu_r$  and  $\mu_F$  are dynamical scales and set to be equal, and we choose  $\mu_0^2 = \frac{1}{4}(m_{\gamma\gamma}^2 + \sum_j p_{T,j}^2)$  for our central scale. When using cone based isolation, the fragmentation scale  $\mu_f$  also enters, and we set it to be equal to the other scales. To assess the effect of a jet veto, we present results for the inclusive and the exclusive case, where for the latter we veto on a second jet by demanding  $p_{T,\text{jet}2} < 30$  GeV. For the photon isolation, we compare the Frixione isolation criterion with the fixed cone criterion for several values of the photon energy fraction  $z_c$  in the cone, where

$$z_c = \frac{|\vec{p}_{T,\text{cone}}^{\text{had}}|}{|\vec{p}_T^\gamma + \vec{p}_{T,\text{cone}}^{\text{had}}|},$$

such that in the collinear limit,  $z_c$  is related to  $\varepsilon_c$  in eq. (2.1) by  $z_c = \frac{\varepsilon_c}{1+\varepsilon_c}$ . For the Frixione isolation criterion (see eq. (2.2)), our default values are  $R = 0.4, n = 1$  and  $\varepsilon = 0.5$ .

We estimate the uncertainty stemming from renormalization, factorization, and, if applicable, fragmentation scale, by varying these scales by a factor of two around the central value. For the exclusive case in Figure 1 we observe a clear reduction in the scale uncertainty whereas for the inclusive case in Figure 2 this is not the case. The reason for this behavior is that real emission contribution dominates the total cross section, therefore leading to a tree level like scale dependence. For the exclusive case this contribution is effectively cut off by the jet veto. However, the smallness of the scale dependence in this case has to be interpreted with care, as this behavior depends on the jet veto and could be due to cancellations which might not be present in all distributions.

Figure 3 shows how the scale variation bands vary as a function of the isolation parameters, for both the single-jet inclusive and the exclusive case. One observes that for both – fixed cone isolation and Frixione isolation – the inclusive case is dominated by the large scale dependence of the  $\gamma\gamma + 2$  jets part of the real radiation which has an uncompensated leading order scale dependence.

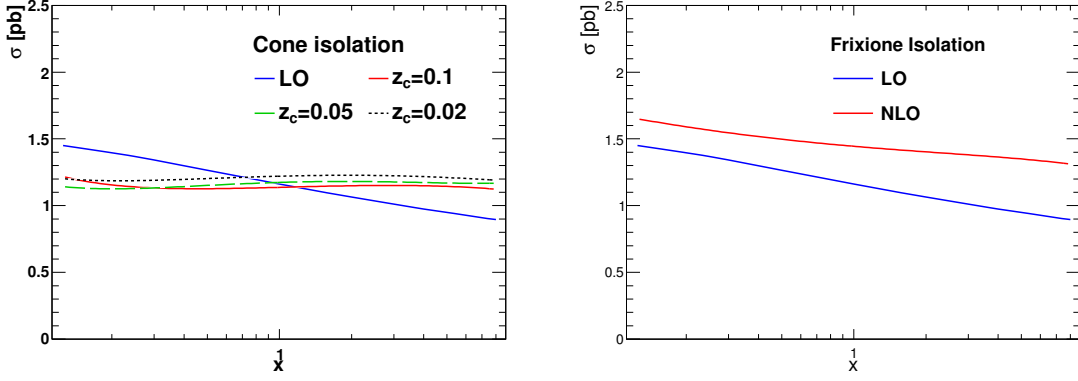


**Figure 1:** Behavior of the exclusive  $\gamma\gamma$ +jet cross sections with different isolation prescriptions under scale variations,  $\mu = x\mu_0$ ,  $0.5 \leq x \leq 2$ ,  $\mu_0^2 = \frac{1}{4}(m_{\gamma\gamma}^2 + \sum_j p_{T,j}^2)$ .

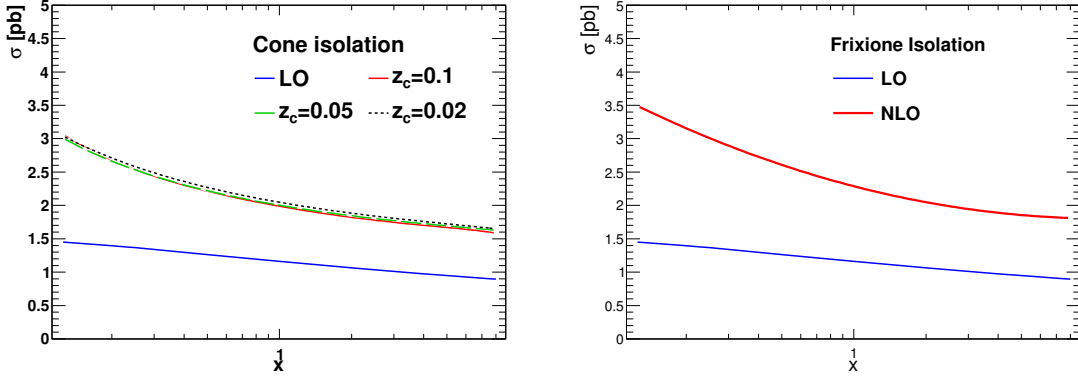


**Figure 2:** Behavior of the inclusive  $\gamma\gamma$ +jet+X cross sections with different isolation prescriptions under scale variations,  $\mu = x\mu_0$ ,  $0.5 \leq x \leq 2$ ,  $\mu_0^2 = \frac{1}{4}(m_{\gamma\gamma}^2 + \sum_j p_{T,j}^2)$ .

#### 4. Diphoton + two jets

For the calculation of a photon pair plus two jets we used the same tools and packages as described in section 3. The calculation has first been described in [33] to which we refer for a more detailed description.

##### 4.1 Numerical results

The numerical results presented in the following have been calculated at a center-of-mass energy of  $\sqrt{s} = 8$  TeV. For the jet clustering we used an anti- $k_T$  algorithm [29] with a cone size of  $R_j = 0.5$  provided by the FastJet package [30]. We used the CT10 set of parton distributions [34] as contained in the CT10.LHgrid set of the LHAPDF library [35] for both LO and NLO contributions and worked with  $N_F = 5$  massless quark flavors. The following kinematic cuts, based on recent experimental studies [4], have been applied:  $p_T^{\text{jet}} > 30$  GeV,  $p_T^{\gamma,1} > 40$  GeV,  $p_T^{\gamma,2} > 25$  GeV,  $|\eta^\gamma| \leq 2.5$ ,  $|\eta^j| \leq 4.7$ ,  $R_{\gamma,j} > 0.5$ ,  $R_{\gamma,\gamma} > 0.45$ . For the photon isolation we restricted ourselves to the Frix-

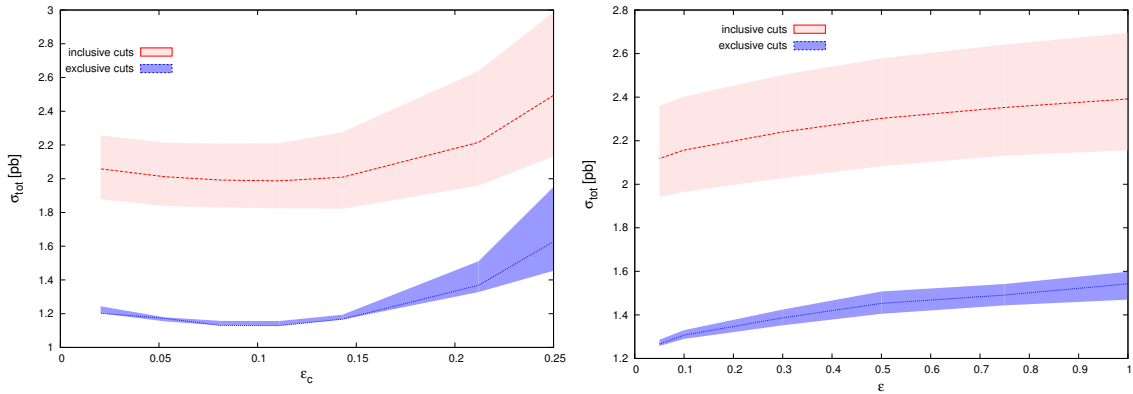


**Figure 3:** Dependence of the cross sections on the cone isolation parameters  $\epsilon_c$  and  $\epsilon$  respectively. The bands correspond to scale variations  $0.5 \leq x \leq 2$ .

isolation criterion with  $R = 0.4$ ,  $n = 1$  and  $\epsilon = 0.05$ . A more detailed analysis with different isolation criteria and various isolation parameters will be presented elsewhere. The scales have been chosen as in section 3. Figure 4 shows the scale variation around the central value. A clear reduction of the scale dependence can be observed by adding the next-to-leading order contributions with a moderate K-factor of  $\sim 1.3$  for the central scale. The effects of the next-to-leading order

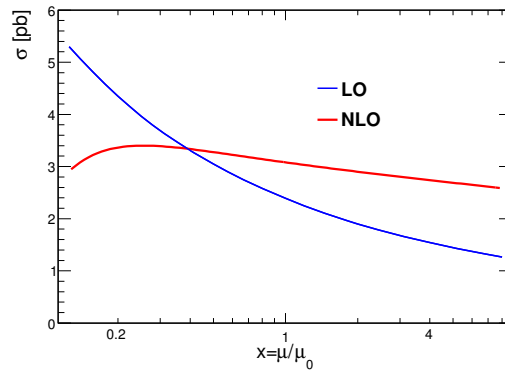


**Figure 4:** Scale dependence of the total cross section at LO and NLO with  $x = \mu/\mu_0$ .

corrections in differential distributions can be substantial even if the effects on the total cross section are rather moderate. This is in particular true, if at NLO, regions in phase space open up that are kinematically not allowed at leading order. Figure 5 shows the  $R$ -separation between the hardest jet and the hardest photon. The colored bands denote the scale uncertainty when varying around the central scale by a factor of two. For small values of  $R$ , the NLO corrections lead to a strong distortion of the shape. This can be understood in terms of kinematically allowed regions. At LO, the pair of hard photon and hard jet being close in  $R$ -space would have to be counterbalanced with the soft photon and the soft jet. This is kinematically impossible at LO but appears at NLO due to the additional radiation.

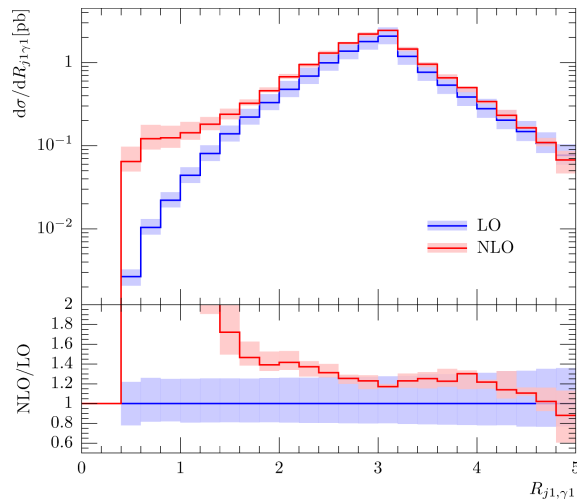


**Figure 5:**  $R$ -separation  $R(j_1, \gamma_1)$  between the hardest jet and the hardest photon.

## 5. Conclusions

We have presented the next-to-leading order QCD corrections to the production of a photon pair in association with one and two jets. This class of processes is important for a reliable prediction of the Standard Model background to the  $H \rightarrow \gamma\gamma$  signal. In the one jet case we have implemented and compared two types of photon isolation criteria, the fixed cone isolation and Frixione isolation. For both cases we find large NLO corrections and for the inclusive case a strong dependence on the scale. The scale dependence can be effectively reduced by imposing a veto on a second jet. In general we find a strong dependence on isolation types and parameters, however it can be observed that for tight isolation parameters, the results obtained with different isolation types approach each other. We also calculated the first NLO corrections to the process of diphoton plus two jet production. For the photon isolation we used Frixione isolation and found moderate NLO corrections to the total cross section. The effects on differential distributions depend on the observable and can lead to strong distortions of the shape.

## Acknowledgments

We thank the other members of the GoSam collaboration for useful discussions. N.G. and G.H. want to thank the University of Zurich for kind hospitality while parts of this project were carried out. This work was supported in part by the Schweizer Nationalfonds under grant 200020-138206, and by the Research Executive Agency (REA) of the European Union under the Grant Agreement number PITN-GA-2010-264564 (LHCPhenoNet). We acknowledge use of the computing resources of the Rechenzentrum Garching.

## References

- [1] G. Aad *et al.* [ATLAS Collaboration], Phys. Lett. B **716** 1 (2012) [arXiv:1207.7214]; S. Chatrchyan *et al.* [CMS Collaboration], Phys. Lett. B **716** 30 (2012) [arXiv:1207.7235].

- [2] [ATLAS Collaboration], ATLAS-CONF-2013-012, ATLAS-CONF-2013-072.
- [3] [CMS Collaboration], CMS-PAS-HIG-13-001, HIG-13-016-pas.
- [4] [CMS Collaboration], CMS-PAS-SMP-13-001.
- [5] J. R. Ellis, M. K. Gaillard and D. V. Nanopoulos, Nucl. Phys. B **106** 292 (1976); M. A. Shifman, A. I. Vainshtein, M. B. Voloshin and V. I. Zakharov, Sov. J. Nucl. Phys. **30** 711 (1979).
- [6] T. Binoth, J. P. Guillet, E. Pilon and M. Werlen, Eur. Phys. J. C **16**, 311 (2000) [hep-ph/9911340].
- [7] S. Catani, L. Cieri, D. de Florian, G. Ferrera and M. Grazzini, Phys. Rev. Lett. **108** 072001 (2012) [arXiv:1110.2375].
- [8] V. Del Duca, F. Maltoni, Z. Nagy and Z. Trocsanyi, JHEP **0304** 059 (2003) [hep-ph/0303012].
- [9] Z. Bern, L. J. Dixon and C. Schmidt, Phys. Rev. D **66**, 074018 (2002) [hep-ph/0206194].
- [10] C. Balazs, P. M. Nadolsky, C. Schmidt and C. P. Yuan, Phys. Lett. B **489**, 157 (2000) [hep-ph/9905551].
- [11] C. Balazs, E. L. Berger, P. M. Nadolsky and C. -P. Yuan, Phys. Lett. B **637**, 235 (2006) [hep-ph/0603037].
- [12] S. Frixione, Phys. Lett. B **429** 369 (1998) [hep-ph/9801442].
- [13] T. Gehrmann, N. Greiner and G. Heinrich, JHEP **1306** 058 (2013) [arXiv:1303.0824].
- [14] T. Stelzer and W. F. Long, Comput. Phys. Commun. **81**, 357 (1994) [hep-ph/9401258]; J. Alwall *et al.*, JHEP **0709**, 028 (2007) [arXiv:0706.2334].
- [15] R. Frederix, T. Gehrmann and N. Greiner, JHEP **0809**, 122 (2008) [arXiv:0808.2128]; R. Frederix, T. Gehrmann and N. Greiner, JHEP **1006**, 086 (2010) [arXiv:1004.2905].
- [16] S. Catani and M. H. Seymour, Nucl. Phys. B **485**, 291 (1997) [Erratum-ibid. B **510**, 503 (1998)] [hep-ph/9605323].
- [17] F. Maltoni and T. Stelzer, JHEP **0302**, 027 (2003) [hep-ph/0208156].
- [18] G. Cullen, N. Greiner, G. Heinrich, G. Luisoni, P. Mastrolia, G. Ossola, T. Reiter and F. Tramontano, Eur. Phys. J. C **72**, 1889 (2012) [arXiv:1111.2034].
- [19] P. Nogueira, J. Comput. Phys. **105**, 279 (1993).
- [20] J.A.M. Vermaseren, math-ph/0010025. J. Kuipers, T. Ueda, J.A.M. Vermaseren and J. Vollinga, Comput. Phys. Commun. **184**, 1453 (2013) [arXiv:1203.6543].
- [21] G. Cullen, M. Koch-Janusz and T. Reiter, Comput. Phys. Commun. **182**, 2368 (2011) [arXiv:1008.0803].
- [22] T. Reiter, Comput. Phys. Commun. **181**, 1301 (2010) [arXiv:0907.3714].
- [23] P. Mastrolia, G. Ossola, T. Reiter and F. Tramontano, JHEP **1008**, 080 (2010) [arXiv:1006.0710].
- [24] R. K. Ellis, W.T. Giele and Z. Kunszt, JHEP **0803**, 003 (2008) [arXiv:0708.2398]. G. Ossola, C.G. Papadopoulos and R. Pittau, Nucl. Phys. B **763**, 147 (2007) [hep-ph/0609007]. P. Mastrolia, G. Ossola, C.G. Papadopoulos and R. Pittau, JHEP **0806**, 030 (2008) [arXiv:0803.3964]. G. Ossola, C.G. Papadopoulos and R. Pittau, JHEP **0805**, 004 (2008) [arXiv:0802.1876]. G. Heinrich, G. Ossola, T. Reiter and F. Tramontano, JHEP **1010**, 105 (2010) [arXiv:1008.2441].

- [25] T. Binoth, J.P. Guillet, G. Heinrich, E. Pilon and T. Reiter, *Comput. Phys. Commun.* **180**, 2317 (2009) [arXiv:0810.0992]. G. Cullen, J.P. Guillet, G. Heinrich, T. Kleinschmidt, E. Pilon, T. Reiter and M. Rodgers, *Comput. Phys. Commun.* **182**, 2276 (2011) [arXiv:1101.5595].
- [26] A. van Hameren, *Comput. Phys. Commun.* **182**, 2427 (2011) [arXiv:1007.4716].
- [27] S. Dittmaier, *Nucl. Phys. B* **565**, 69 (2000) [hep-ph/9904440].
- [28] T. Gehrmann and N. Greiner, *JHEP* **1012**, 050 (2010) [arXiv:1011.0321 [hep-ph]].
- [29] M. Cacciari, G. P. Salam and G. Soyez, *JHEP* **0804**, 063 (2008) [arXiv:0802.1189].
- [30] M. Cacciari and G. P. Salam, *Phys. Lett. B* **641**, 57 (2006) [hep-ph/0512210]. M. Cacciari, G. P. Salam and G. Soyez, *Eur. Phys. J. C* **72**, 1896 (2012) [arXiv:1111.6097].
- [31] R. D. Ball, V. Bertone, S. Carrazza, C. S. Deans, L. Del Debbio, S. Forte, A. Guffanti and N. P. Hartland *et al.*, *Nucl. Phys. B* **867**, 244 (2013) [arXiv:1207.1303 [hep-ph]].
- [32] L. Bourhis, M. Fontannaz and J. P. Guillet, *Eur. Phys. J. C* **2**, 529 (1998) [hep-ph/9704447].
- [33] T. Gehrmann, N. Greiner and G. Heinrich, arXiv:1308.3660 [hep-ph], *Phys. Rev. Lett.*, to appear.
- [34] H. -L. Lai *et al.*, *Phys. Rev. D* **82**, 074024 (2010) [arXiv:1007.2241].
- [35] M.R. Whalley, D. Bourilkov and R.C. Group, hep-ph/0508110.